Physicochem. Probl. Miner. Process., 55(1), 2019, 128-139

http://www.journalssystem.com/ppmp

Physicochemical Problems of Mineral Processing

ISSN 1643-1049

Received date June 28, 2018; reviewed; accepted October 12, 2018

Characterization of amino-, epoxy- and carbonyl-functionalized halloysite and its application in the immobilization of aminoacylase from *Aspergillus melleus*

Agnieszka Kołodziejczak-Radzimska, Teofil Jesionowski

Poznan University of Technology, Faculty of Chemical Technology, Institute of Chemical Technology and Engineering, Berdychowo 4, PL-60965, Poznan, Poland

Corresponding author: agnieszka.kolodziejczak-radzimska@put.poznan.pl

Abstract: Functionalized halloysite was used as a support for the immobilization of an enzyme. The surface of halloysite was modified with amino (–NH), epoxy (–C(O)C) and carbonyl (–C=O) groups. Both unmodified and modified forms of the support underwent a comprehensive physicochemical and structural evaluation, including morphological, structural, thermogravimetric and spectroscopic analysis. Aminoacylase from *Aspergillus melleus* was used as the enzyme in the immobilization process. The process of immobilization by adsorption was performed for 1, 6 and 24 h using different concentrations of enzyme solution (0.5, 1 and 3 mg/cm^3). The quantity of aminoacylase loaded onto the support was calculated by the Bradford method. Free and immobilized aminoacylase were used to catalyze the deacetylation of *N*-acetyl-L-methionine. Additionally, the thermal and chemical stability of the obtained biocatalytic systems were evaluated, as well as the reusability of the immobilized systems. The biocatalytic system with amino groups demonstrated activity above 70% in the pH range 4–9 and 60% in the temperature range 30–70 °C. Aminoacylase immobilized on amino-functionalized halloysite also retains around 50% of its initial activity after five reaction cycles.

Keywords: functionalized halloysite, physicochemical and structural evaluation, immobilization, thermal and chemical stability, reusability

1. Introduction

Halloysite (HA, $Al_2Si_2O_5(OH)_4 \cdot nH_2O$) is a polymorphic modification of kaolinite, with an extra water molecule between the aluminum oxide and silica layers. It was first described by Beither (1926) as a mineral consisting of tetrahedral SiO_4 sheet stacked with an edge-shared octahedral AlO_6 sheet with an internal aluminol group Al–OH (Yuan et al., 2015; Zhang et al., 2016; Erpek et al., 2017). The halloysite structure and its unique properties make it attractive for applications in polymeric nanocomposites, drug release and biomedical applications (Terzopoulou et al., 2018). Halloysite was formed as a result of natural hydrothermal and weather processes, mainly weathering of rocks, and also in magmatic and nonmagmatic rocks. It therefore occurs in wet tropical and subtropical regions (Cavallaro et al., 2011; Abdullayev et al., 2013).

Among the various phyllosilicate nanomaterials (having a silicate-based layer structure) such as kaolin and montmorillonite, halloysite has distinct advantages. HA contains two types of hydroxyl groups, inner and outer, which are situated respectively between the layers and on the surface of the nanotubes (Du et al., 2010; Massaro et al., 2017). Due to the multi-layer structure, most of the hydroxyl groups are inner groups, only a few being located on the surface of the halloysite. This makes HA relatively hydrophobic, which enables its easy dispersion in non-polar polymers, while the other hydroxyl groups present on the surface provide active sites for chemical functionalization. The nanotubular structure also makes HA an excellent carrier for biologically active substances (Lvov et al., 2016; Zhu et al., 2017).

DOI: 10.5277/ppmp18180

Halloysite is a natural nanomaterial with a unique combination of a hollow tubular nanostructure, large aspect ratio, mechanical strength, broad potential in terms of functionality, biocompatibility, and availability in large amounts at low cost. In addition, halloysite is proven to be a biocompatible and ecofriendly material, as shown by several *in vitro* and *in vivo* studies (Gaaz et al., 2017). Due to its large specific surface area, high biocompatibility and nanotubular structure, it is used as a support material. It has been widely used for studies of the loading and controlled release of various substances, ranging from low-molecular-mass organic molecules to complex biochemical molecules (Yuan et al., 2015). The following enzymes have been immobilized on halloysite: amylase (Pandey et al., 2017; Zhai et al., 2010), horseradish peroxidase (Kim et al., 2012), urease (Zhai et al., 2010), laccase (Kadam et al., 2017; Tully et al., 2016), glucose oxidase (Kumar-Krishnan et al., 2016; Tully et al., 2016) and lipase (Tully et al., 2016).

Aminoacylase (EC 3.5.1.14) is a complex protein whose active center consists of one or two related zinc atoms. This enzyme is a hydrolase, and catalyzes the asymmetric hydrolysis of *N*-acetyl-DL-amino acids to L-amino acids (Youshko et al., 2004; Vaidya et al., 2012; Kolodziejczak-Radzimska et al., 2018). Aminoacylase occurs in various plants, animals and microorganisms. The most often used aminoacylases are from porcine kidney and microorganisms (such as *Aspergillus oryzae, Aspergillus melleus, Pyrococcus furiosus, Thermococcus litoralis*). Aminoacylases from *Aspergillus sp*. are ideally suited as catalysts in industrial processes. Above all they are inexpensive and relatively stable. For a long time, aminoacylase isolated from *Aspergillus* fungi have been widely used for the industrial production of natural (for example: L-alanine, L-methionine, L-valine) and artificial (for example: L-α-aminobutyric acid, L-norvaline, L-norleucine) amino acids (Toogood et al., 2002; Dong et al., 2010).

In the present work, for the first time, the aminoacylase from *Aspergillus melleus* was immobilized onto amino- (–NH), epoxy- (–C(O)C–) and carbonyl- (–C=O) functionalized halloysite. The supports used underwent morphological (TEM, SEM), structural (BET), spectroscopic (FTIR) and thermogravimetric (TG/DTG) analysis. The resulting biocatalytic systems were used to catalyze the hydrolysis of *N*-acetyl-L-methionine. The influence of enzyme concentration (mg/cm^3) and time of immobilization (h) on the quantity of enzyme loaded (mg/g) was determined. The effectiveness of the immobilization process was indirectly confirmed by spectroscopic analysis (FTIR and Raman). The chemical (pH=4–9) and thermal (30–70 °C) stability of aminoacylase immobilized on functionalized halloysite was also evaluated. Additionally, the reusability of the biocatalytic systems after immobilization was verified based on the same hydrolysis reaction.

2. Materials and methods

2.1. Materials

Halloysite (HA) was purchased from PTH INTERMARK (powder with reduced iron content, from the Dunino mine). 3-aminopropyltriethoxysilane (APTES), 3-glycidyloxypropyltrimethoxysilane (GPTES), aminoacylase I from *Aspergillus melleus* (AAM), *N*-acetyl-L-methionine (*AcMet*), ninhydrin reagent, methanol and ethanol were purchased from Sigma Aldrich (St. Louis, MO). Glutaraldehyde (GA) was obtained from Amresco (Solon, OH). Monobasic sodium phosphate (NaH_2PO_4) and dibasic sodium phosphate (Na_2HPO_4), sodium acetate (CH_3COON_a), acetic acid (CH_3COOH), hydrogen chloride (HCl) and tris(hydroxymethyl)aminomethane (Tris), obtained from Sigma Aldrich (St. Louis, MO), were used to prepare the buffer solution. All chemicals were of analytical grade and were used as received without any further purification.

2.2. Modification of halloysite with amino, epoxy and carbonyl groups

Modification was performed using a "dry method" (Jesionowski et al., 2001). In the first step the silane coupling agents (3-aminopropyltriethoxysilane and 3-glycidyloxypropyltrimethoxysilane; 3 wt./wt.) were hydrolyzed in a methanol/water system (4:1, v/v) and then sprayed directly onto the halloysite surface. The products were then dried for 2 h at 105 °C. The prepared samples were denoted HA_A (halloysite modified with amino groups) and HA_E (halloysite modified with epoxy groups).

In the next step, pristine halloysite and amino-functionalized halloysite were crosslinked with glutaraldehyde. A defined quantity of support was immersed in a 5% solution of glutaraldehyde, and

the system was shaken for 24 h at ambient temperature. This sample was denoted HA_GA (halloysite modified with carbonyl groups).

2.3. Physicochemical and structural evaluation

Morphology and microstructure were investigated using a Jeol 1200 EX II transmission electron microscope and a Zeiss VO40 scanning electron microscope. Particle size distribution was measured with a Mastersizer 2000 using laser diffraction (Malvern Instruments Ltd., UK). Additionally, low-temperature N_2 sorption was applied. The surface area (A_{BET}), total pore volume (V_p) and average mean size (S_p) were determined using an ASAP 2020 instrument (Micromeritics Instrument Co., USA). To identify the characteristic groups present on the surface of the products, the samples were subjected to FTIR analysis using a Vertex 70 spectrophotometer (Bruker, Germany). A thermogravimetric analyzer (TG, model Jupiter STA 449F3, made by Netzsch, Germany) was used to investigate the thermal decomposition behavior of the samples. The zeta potential of the obtained materials was determined as a function of pH, using a Zetasizer Nano ZS equipped with an autotitrator (Malvern Instruments Ltd., UK), which enables measurement of electrophoretic mobility, and indirectly of the zeta potential, based on laser Doppler velocimetry. All of these analyses are described in detail in previously published papers (Kolodziejczak-Radzimska, 2010, 2017, 2018).

The Raman scattering spectra were investigated within a spectral range of 3500–250 cm^{-1}. The non-polarized Raman spectra were recorded in a back scattering geometry, using the in Via Renishaw micro-Raman system (New Mills, UK). The in Via Raman spectrometer enabled the recording of Raman spectra with a spatial resolution of about 1 m. The spectral resolution was 4 cm^{-1}. A laser operating at 520 nm was used as excitation light. The elemental composition of the materials was established with the use of a Vario El Cube instrument (Elementar Anlaysensysteme GmbH, Germany), which gave the elemental contents (weight percent) of carbon, nitrogen and hydrogen after high temperature combustion of the analyzed samples. Results are given as averages for three measurements, each accurate to ±0.0001%.

2.4. Immobilization process and activity assay of obtained biocatalytic systems

Aminoacylase was dissolved in phosphate buffer (PBS 0.2 M, pH 7) with various initial aminoacylase concentrations (0.5, 1 and 3 mg/cm^3; pH 7). Then 1 g of functionalized halloysite was added, and the immobilization process was performed at ambient temperature for 1, 6 and 24 h. After filtering, the precipitate was dried at ambient temperature for 24 h. The activity of the immobilized aminoacylase was measured, and the optimal aminoacylase concentration or immobilization time was determined accordingly. The quantity of AAM immobilized was determined via the Bradford method (BRADFORD, 1976) using BSA as a reference. It was calculated from equation (1):

$$P = \frac{(C_0 - C_1) \cdot V}{m} \quad [\frac{mg}{g}] \tag{1}$$

where P is the quantity of the enzyme (mg/g), C_0 and C_1 denote the concentration of the enzyme (mg/cm^3) in solution before and after immobilization respectively, V is the volume of solution (cm^3), and m is the mass of modified $MgO{\cdot}SiO_2$ (g).

To evaluate the stability of the bonds between the enzyme molecules and the supports, and the potential reuse of the immobilized enzyme, desorption tests were performed using selected samples of functionalized halloysite with enzyme (obtained using the higher concentration of enzyme). Desorption was calculated from equation (2):

$$D = \frac{C_a}{C_d} \cdot 100\ [\%] \tag{2}$$

where C_a is the amount (concentration) of the enzyme that was immobilized (according to the efficiency of immobilization) and C_d is the concentration of the enzyme that was removed from the support surface during the desorption tests (mg/cm^3).

The assay of aminoacylase activity with *AcMet* as substrate, and the calculation of the relative activity of aminoacylase immobilized on the functionalized halloysite, were performed in the same way as in our previous study (Kolodziejczak-Radzimska, 2018).

2.5. Stability of activity of free and immobilized aminoacylase

The thermal and chemical stability of the native enzyme and the immobilization products were evaluated in the pH range 4–9 and the temperature range 30–70 °C. The catalytic activity was determined based on the reaction of detection of amino acid in the presence of ninhydrin reagent (Kolodziejczak-Radzimska, 2018).

2.6. Reusability of aminoacylase immobilized on halloysite

The activity measurement was performed for 5 reaction cycles. After the reaction the enzyme was separated, dried and reused in the hydrolysis reaction.

All measurements were made in triplicate, and results are presented as means ±3.0 SD.

3. Results and discussion

3.1. Characterization of prepared supports (unmodified and modified halloysite)

Fig. 1 presents basic physicochemical and structural characteristics of unmodified halloysite. According to the particle size distribution (Fig. 1a), the mineral sample contains 90% of particles with diameters smaller than 13.2 µm, 50% of particles smaller than 10.1 µm, and 10% of particles not greater than 6.1 µm. The measured mean particle diameter of this sample is 8.9 µm. Fig. 1b shows an SEM image of the halloysite, which confirms the presence of nano- and micrometric sized particles. The TEM image (Fig. 1c) shows that the material contains primary particles with a homogeneous structure and diameters below 500 nm, which tend to agglomerate, as confirmed by previously reported results.

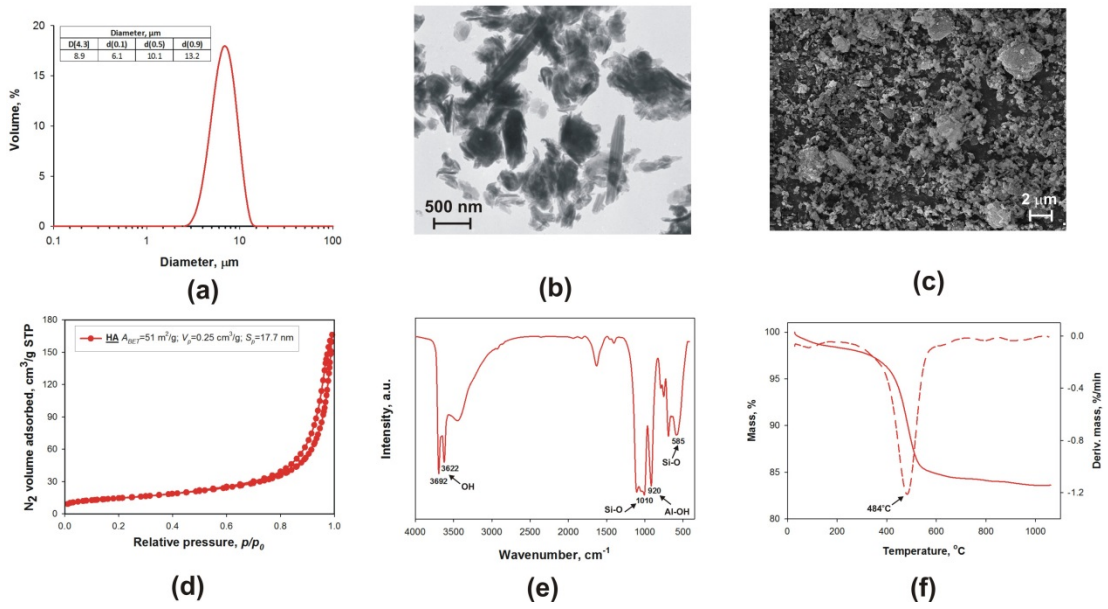

Fig. 1. (a) Volume contributions for particles with diameters in the range 0.02–2000 µm, (b) TEM image, (c) SEM image, (d) nitrogen adsorption/desorption isotherm, (e) FTIR spectrum and (f) TG/DTG curves of unmodified halloysite

The halloysite also has a well-developed porous structure, as can be seen in Fig. 1d. The isotherms (Fig. 1d) were classified as type IV and the hysteresis loops as type H3, which points to the mesoporous structure of the modified silica. Halloysite has a specific surface area of 51 m^2/g, an mean pore diameter of 17.7 nm and a total pore volume of 0.25 cm^3/g. Thanks to its well-developed porous structure, the halloysite can be classed as a potential support for immobilization processes. In the FTIR spectrum of HA (Fig. 1e) the absorption bands at 3692 and 3622 cm^{-1} are attributed to −OH groups. The band at 920 cm^{-1} is attributed to bending vibrations of Al−OH, and the bands at 1010 and 585 cm^{-1} to Si−O stretching and bending vibrations respectively (Chao, 2013). To determine the change in mass of halloysite particles as a function of temperature, TG/DTG was conducted. The results (Fig. 1f) indicate that

halloysite remains relatively stable up to 400 °C. Above 484 °C there is a mass loss of 15%, attributed to dehydration due to the removal of interlayer water (Gaaz, 2017; Deng, 2008).

The FTIR analysis confirmed the presence on the halloysite surface of –OH, Al–OH and Si–O groups, which enable the process of modification with amino, epoxy and carbonyl groups. TG/DTG, FTIR, BET and elemental analysis were performed to confirm the modification process. The results are shown in Fig. 2 and Table 1.

The FTIR spectra of modified halloysite (Fig. 2a) contain bands originating from the halloysite and from the modifiers. Stretching vibrations of –C–H, characteristic for the aliphatic chains of the modifiers, appear in the wavenumber range 2900–2800 cm^{-1}, indicating that the modifying agent was successfully attached to the surface of the support. There are also signals related to functional moieties contained in the structure of the modifiers, such as a peak at 1456 cm^{-1} in the spectrum of HA_A (stretching vibrations of –C–N bonds), a signal with a maximum around 695 cm^{-1} in the spectrum of HA_E (deformational vibrations of epoxy rings) and bands around 1729 cm^{-1} in the spectrum of HA_GA (stretching vibrations of –C=O). The presence of these groups in the analyzed samples confirms the effectiveness of the surface functionalization.

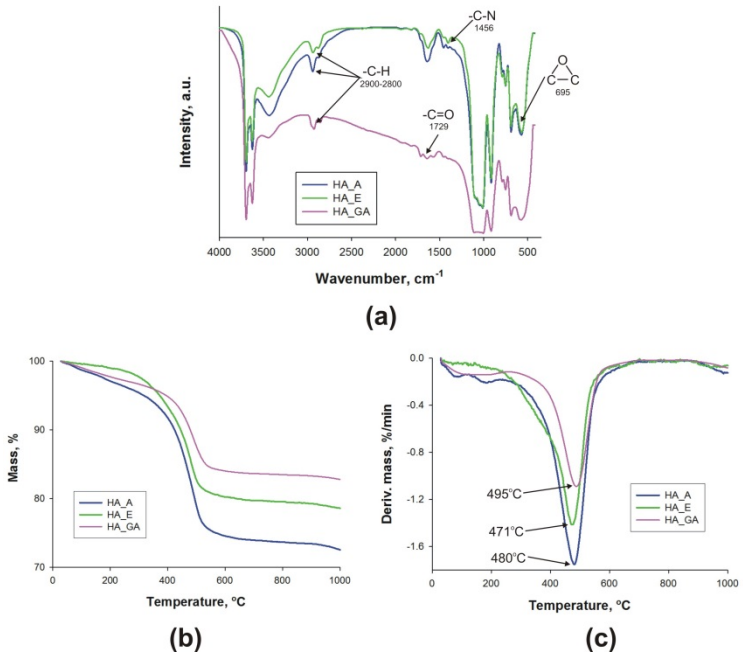

Fig. 2. (a) FTIR spectra, (b) TG and (c) DTG curves of functionalized halloysite

The modification process did not significantly affect the thermal stability of halloysite, as was confirmed by TG/DTG analysis (Fig. 2b, c). The obtained systems are stable up to 450 °C; above this temperature the samples lost about 15%, 20% and 25% of their initial mass respectively for carbonyl- (HA_GA), epoxy- (HA_E) and amino-functionalized halloysite (HA_A). The porous structure parameters and contents of nitrogen, carbon and hydrogen (Table 1) also confirm the effectiveness of the modification process. The data in Table 1 indicate that modification led to a decrease in surface area (15 m^2/g for HA_A, 17 m^2/g for HA_E, 16 m^2/g for HA_GA), pore volume (0.01 cm^3/g for HA_A, HA_E and HA_GA) and pore diameter (2.9 nm for HA_A and HA_E, 3.0 nm for HA_GA). Additionally, the samples after modification had increased contents of carbon (10.08% for HA_A, 5.13% for HA_E, 3.01% for HA_GA) and hydrogen (2.42% for HA_A, 1.77% for HA_E, 1.55% for HA_GA), and the appearance of nitrogen (1.79%) was observed in the halloysite modified with amino groups (HA_A).

The next stage in the physicochemical analysis was to study changes in zeta potential as a function of pH. Figure 3 presents the electrokinetic curves measured for unmodified and modified supports. The electrokinetic curve for the unmodified halloysite (HA) shows that the zeta potential for this sample is negative in whole analyzed pH range. Whereas, the zeta potential values for the modified halloysite (HA_A, HA_E and HA_GA) is significantly different. Modified supports are characterized with zeta

potential of 18–(-41.7) mV (HA_A), 6.5–(-42.7) mV (HA_E) and -2.5–(-42.4) mV in different pH. Moreover, shift in the IEP (isoelectric point) value 6.57 and 1.86 for HA_A and HA_E accordingly, was observed. Significantly changes in value of zeta potential for modified halloysite results from the nature of interaction as well as type of functional groups present in modifiers.

Table 1. Porous structure parameters and elemental contents of unmodified and modified halloysite

Acronym of sample	Parameters of porous structure			Content (%)		
	A_{BET} (m^2/g)	V_p (cm^3/g)	S_p (nm)	N	C	H
HA	51	0.25	17.7	-	1.93	1.20
HA_A	15	0.01	2.9	1.79	10.08	2.42
HA_E	17	0.01	2.9	-	5.13	1.77
HA_GA	16	0.01	3.0	-	3.00	1.56

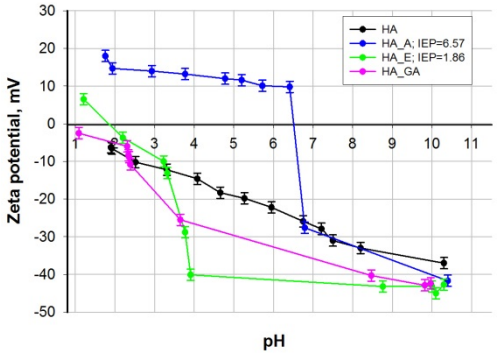

Fig. 3. Zeta potential values as a function of pH and values of IEP for the unmodified and modified halloysite

3.2. Evaluation of the effectiveness of immobilization of aminoacylase on amino-, epoxy- and carbonyl-functionalized halloysite

The amino-, epoxy- and carbonyl-functionalized halloysites (HA_A, HA_E and HA_GA) were used as supports in the immobilization of aminoacylase from *Aspergillus melleus*. The effectiveness of immobilization was indirectly confirmed by FTIR spectra (Fig. 4), which contain bands generated by the vibrations of groups present on the modified halloysite surface and in the enzyme structure.

The most important bands present on the spectrum of free aminoacylase correspond to stretching vibrations of $-NH_2$ (3270 cm^{-1}) and C–H (2934 cm^{-1}) and vibrations of amide I and III bonds (1659 and 1451 cm^{-1} respectively). The effective immobilization of aminoacylase on the modified halloysite is confirmed by the bands in the wavenumber range 1700–1400 cm^{-1}, which indicate the presence of amide I and III bonds. The intensity of these peaks is lower than on the spectrum of free aminoacylase (Kolodziejczak-Radzimska et al., 2018).

Raman spectroscopy can provide important information to explain the effect of physical and chemical treatments as well as the interfaces between the support and the immobilized enzyme. Fig. 5 shows Raman spectra for the pure supports (H_A, H_E and H_GA) and the obtained biocatalytic systems (H_A_AAM, H_E_AAM and HA_GA_AAM). These spectra are shown in the range 1800–1000 cm^{-1}, because this range contains the characteristic bands confirming the presence of the enzyme on the support surface. Characteristic peaks for amide I and amide III are observed at 1634–1690 cm^{-1} and 1245–1270 cm^{-1} respectively on the spectra of HA_A_AAM and HA_E_AAM; they are not present on the spectra of the supports. In the case of aminoacylase immobilized on HA_E an amide III band was also found at 1580 cm^{-1}. The higher intensities of the peaks provide confirmation of the chemical changes taking place following immobilization. Similar observations have been reported in previous studies (Orregro, 2010; Elias, 2018).

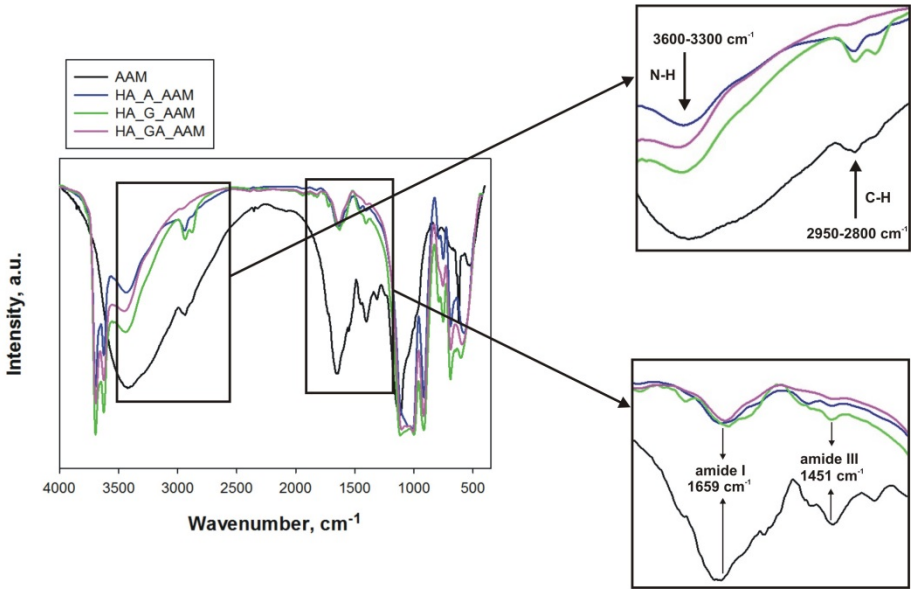

Fig. 4. FTIR spectra of free aminoacylase and aminoacylase immobilized on modified halloysite

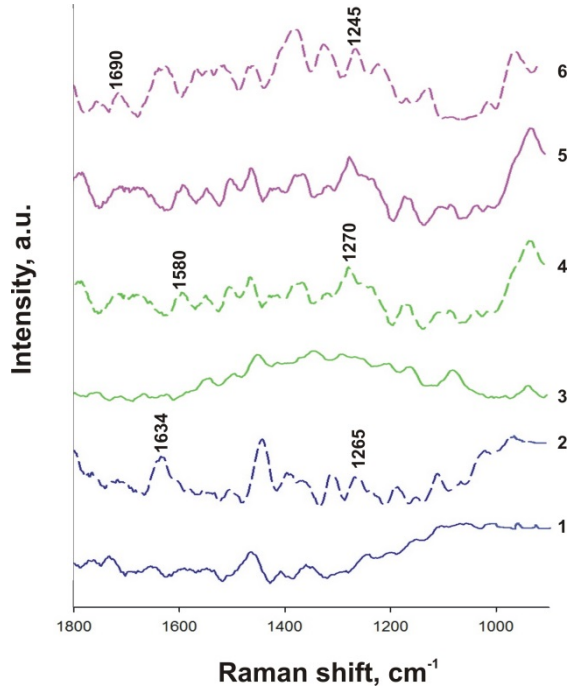

Fig. 5. Raman spectra of supports and immobilized aminoacylase systems: 1 – HA_A, 2 – HA_A_AAM, 3 – HA_E, 4 – HA_E_AAM, 5 – HA_GA and 6 – HA_GA_AAM

After immobilization, the changes were also observed in zeta potential values and value of isoelectric point. Native aminoacylase has its isoelectric point at pH=2.27, and its zeta potential ranges from 1.7 to 25.7 mV over the studied pH range (see Fig. 6). Immobilization of aminoacylase caused some changes in the zeta potential values estimated in different pH as compared to raw supports. The zeta potential values of AAM immobilized onto HA_A (halloysite modified with amine groups) are slightly different in comparison to supports (17–(-48.1) mV). Significantly change is observed for the isoelectric point, which value is decreasing (IEP=3.89). It can be probably connected with the $-NH_2$ groups presents on the support surface, which after immobilization create the amide group with the –COOH groups from enzyme surface. Sample HA_E_AAM is characterized with zeta potential range of 2.1–(-34.7) mV. Furthermore, shift in the IEP value (pH=1.47) for this sample was observed. The zeta potential curves of the HA_E_AAM and HA_GA_AAM samples are slightly different. The electrokinetic curve for the

HA_GA_AAM shows that the zeta potential for this sample is negative in whole analyzed pH range. The changes observed in zeta potential and isoelectric point value suggest that immobilization of aminoacylase significantly affect the surface charge of the support.

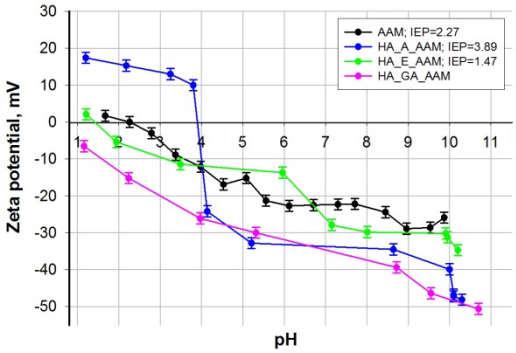

Fig. 6. Zeta potential values as a function of pH and values of IEP for the free and immobilized aminoacylase

3.3. Performance of the immobilization process

Results for quantities of aminoacylase loaded on halloysite (mg/g) are given in Table 2. These data show that the quantity immobilized increases with an increase in the enzyme concentration, whereas the time of the immobilization process has no significant effect on this value. The type of support used also does not affect the quantity of immobilized enzyme, which lies in the range 176–178 mg/g (for the highest concentration of enzyme). Comparison of the data obtained with other data reported in the literature indicates that satisfactory results were obtained. Kadam et al. (2017) obtained 84.26 mg/g laccase loading on supermagnetic halloysite functionalized with aminosilane, and Chao et al. (2013) used halloysite modified with dopamine to immobilize laccase, obtaining a loading capacity of 168 mg/g.

Table 2. Quantities of aminoacylase loaded on halloysite (mg/g) and desorption tests (%)

Support	Time (h)	Concentration of enzyme (mg/cm³)			Desorption*	
		0.5	1	3	Test number	%
		Amount of enzyme ($mg_{enzyme}/g_{support}$)				
HA_A	1	30	60	177	I	0.02
	6	30	60	**(178)***	II	0.03
	24	29	59	178	III	0.10
HA_G	1	29	58	176	I	0.04
	6	29	58	**(177)***	II	0.10
	24	28	57	176	III	0.33
HA_GA	1	29	58	176	I	2.98
	6	28	57	**(177)***	II	2.71
	24	29	60	170	III	3.11

* The desorption test was made for samples marked by **( )***

The possibility of reusing the immobilized enzyme multiple times increases the attractiveness of the process of immobilization by adsorption. The purpose of the desorption tests was to establish the stability of the combination of aminoacylase with the functionalized halloysite. Table 2 contains experimental data concerning the efficiency of desorption of the enzyme from samples obtained during the immobilization process. The obtained systems exhibited high stability: the desorption of the enzyme did not exceed 0.1% (for sample H_A_AAM), 0.4% (for sample HA_G_AAM) and 4% (for sample HA_GA_AAM). This is closely related to the efficiency of adsorption of the enzyme and its different interactions with the functionalized halloysite. The very low rate of desorption of the enzyme may be

proof of its chemisorption onto the surface of the functionalized halloysite (Cisielczyk, 2017). These findings were also confirmed by spectroscopic analysis (FTIR and Raman).

3.4. Evaluation of the activity of free aminoacylase and aminoacylase immobilized on modified halloysite

Free aminoacylase and the same enzyme immobilized on modified halloysite were used to catalyze the deacetylation of *N*-acetyl-L-methionine. On the basis of this reaction the relative activity of the biocatalytic systems at different pH (4–9) and temperature (30–70 °C) was determined. Free AAM is a homogeneous catalyst, whereas the immobilized AAM becomes a heterogeneous catalyst. Therefore, the reusability of the obtained biocatalytic systems was also verified. The results are presented in the form of graphs in Fig. 7.

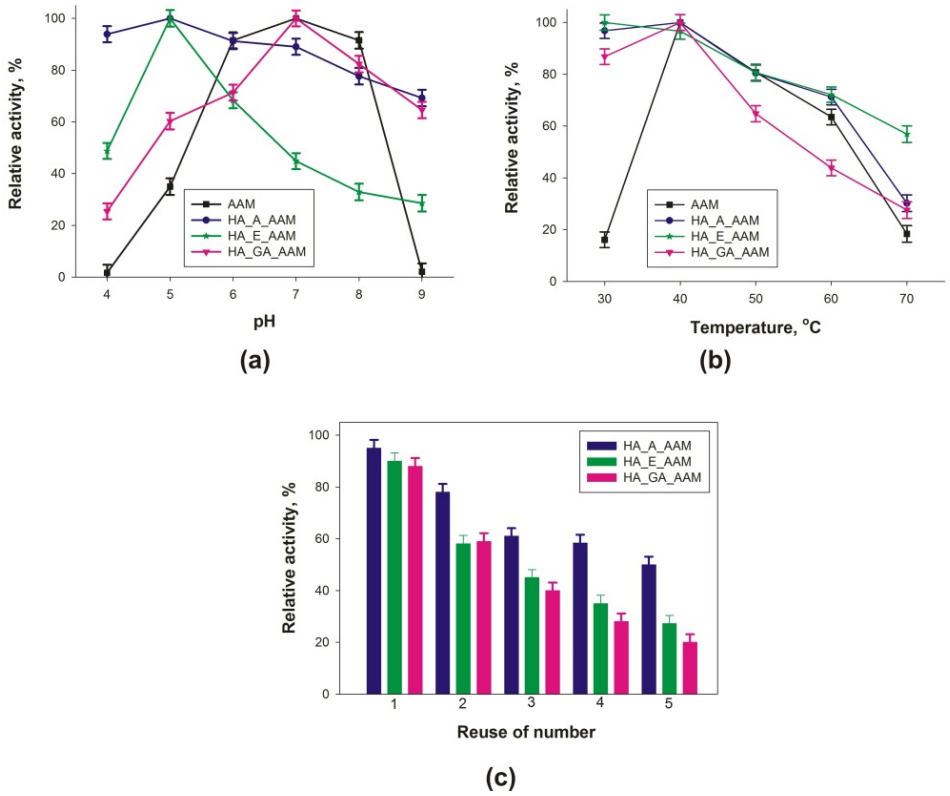

Fig. 7. Effect of (a) pH and (b) temperature on the activity of free and immobilized aminoacylase, and (c) reusability of the obtained biocatalytic systems

As can be seen from Fig. 7a, aminoacylase immobilized on amino-, epoxy- and carbonyl-functionalized halloysite is more stable than the free enzyme over the whole of the analyzed pH range. The free enzyme exhibits its highest activity in the pH range 6–8; in a more acidic or more basic environment its activity falls markedly (to below 10%). The greatest stability (above 70%) over the whole analyzed pH range is demonstrated by aminoacylase immobilized on halloysite modified with amino groups (HA_A_AAM). Somewhat poorer values of relative activity were obtained for the systems HA_E_AAM (halloysite with epoxy groups; above 30%) and HA_GA_AAM (halloysite with carbonyl groups; above 20%). According to literature reports, α-amylase immobilized on halloysite exhibits an activity above 40% in the same pH range (Pandey, 2017), while horseradish peroxide (HRP) immobilized on halloysite has an activity above 60% (Kim, 2012).

The immobilized systems also retain higher catalytic activity than pure aminoacylase over the analyzed temperature range (30–70 °C) (Fig. 7b). The free enzyme exhibits its greatest activity at 40 °C; its activity falls markedly above or below that temperature. However, the catalytic activity of the immobilized systems remains at 80% at temperatures below 40 °C. Above 40 °C the activity of the system HA_E_AAM (epoxy-functionalized halloysite) remains at a fairly high level, above 60%,

although for HA_A_AAM (amino-functionalized halloysite) and HA_GA_AAM (carbonyl-functionalized halloysite) the activity falls to 20%. Similar findings were reported by Kim et al. (2012) and Pandey et al. (2017).

As noted above, immobilization leads to heterogeneous catalysts. From the point of view of practical applications, it is extremely important to determine the reusability of the immobilized enzyme. Fig. 7c shows the catalytic activity of the systems after five reaction cycles. The data show that the system HA_A_AAM (amino-functionalized halloysite) retains 50% of its initial activity; for HA_E_AAM (epoxy-functionalized halloysite) and HA_GA_AAM the results were 30% and 20% respectively. This observation is in agreement with previously reported results on the immobilization of α-amylase and urease (Zhai, 2010), where the immobilized enzyme retained over 60% of its initial activity after five cycles.

Overall, the evaluation of the stability of free and immobilized aminoacylase showed the best system to be that in which aminoacylase was immobilized on amino-functionalized halloysite. This may be because in that system stable bonds were formed between the enzyme and the support surface, as is confirmed by the spectroscopic analysis and desorption tests.

4. Conclusions

An organofunctionalized halloysite has been shown to be a suitable support for the immobilization of aminoacylase from *Aspergillus melleus*. Morphological analysis of the pure halloysite shows that it contains particles of nano- and micrometric size. The well-developed porous structure (A_{BET}=51 m^2/g, S_p=17.7 nm and V_p=0.25 cm^3/g) and the presence on the surface of characteristic functional groups (–OH, Al–OH and Si–O) enabled the modification of the substance with amino, epoxy and carbonyl groups. The effectiveness of the modification process was confirmed by the results of spectroscopy, porous structure analysis and elemental analysis. The FTIR spectra of the modified systems contain bands originating both from pure halloysite and from characteristic groups present in the structure of the modifiers (–C–H, –C–N, –C=O and –C(O)C). The success of the modification is also confirmed by the reduction in the specific surface area (15–17 m^2/g), pore diameter (2.9–3.0 nm) and pore volume (0.01 cm^3/g), suggesting that the modifier is deposited in the interior of the pores. Moreover, the modified systems contained greater quantities of carbon and hydrogen, and nitrogen was observed in the sample HA_A_AAM (aminoacylase on amino-functionalized halloysite). All of the proposed supports demonstrate good thermal stability at high temperatures (TG/DTG analysis). According to the data confirming the effectiveness of the immobilization process, the quantity of aminoacylase immobilized is 176–178 mg per gram of support, irrespective of the type of functional groups present on the surface of the halloysite. The presence of bands corresponding to amide groups on the FTIR and Raman spectra of the immobilized systems indirectly confirms the effectiveness of the immobilization. The changes observed in zeta potential and isoelectric point value also confirm the effectiveness of the immobilization. The obtained biocatalytic systems also exhibit greater chemical and thermal stability than the native enzyme. The highest levels of activity, above 70% over the whole analyzed pH range of 4–9 and above 60% over the temperature range 30–70 °C, were recorded for aminoacylase immobilized on amino-modified halloysite. This system also retains 50% of its initial activity after five reaction cycles.

Acknowledgments

This research was founded by Ministry of Science and Higher Education (Poland) as financial subsidy to PUT

References

ABDULLAYEV E., LVOV Y., 2013. *Halloysite clay nanotubes as a ceramic „skeleton" for functional biopolimer composites with sustained drug release*, J. Mater. Chem. B 1, 2894-2903.

BRADFORD M. M., 1976. *A rapid and sensitive method for the quantitation of microgram quantities of protein utilizing the principle of protein-dye binding*, Anal. Biochem. 72, 248-254.

CAVALLARO G., LAZZARA G., MILIOTO S., 2011. *Dyspersion of nanoclays of different shapes into aqueous and solid biopolymeric matrices. Extended physicochemical study*, Langmuir 27, 1158-1167.

CHAO C., LIU J., WANG J., ZHANG Y., ZHANG B., ZHANG Y., XIANG X., CHEN R., 2013. *Surface modification of halloysite nanotubes with dopamine for enzyme immobilization*, ACS Appl. Mater. Interfaces 5, 10559-10564.

CIESIELCZYK F., BARTCZAK P., ZDARTA J., JESIONOWSKI T., 2017. *Active MgO-SiO_2 hybrid material for organic dye removal: a mechanism and interaction study of the adsorption of C.I. Acid Blue 29 and C.I. Basic Blue 9*, J. Environ. Manage. 204, 123-135.

DENG S., ZHANG J., YE L., WU J., 2008. *Toughening epoxies with halloysite nanotubes*, Polymer 49, 5119-5127.

DONG T., ZHAO L., HUANG Y., TAN X., 2010. *Preparation of cross-linked aggregates of aminoacylase from Aspergillus melleus by using bovine serum albumin as an inert additive*. Bioresource Technol. 101, 6569-6571.

DU M., GUO B., JIA D., 2010. *Newly emerging applications of halloysite nanotubes: a review*, Polym. Int. 59, 574-582.

ELIAS N., CHANDREN S., RAZAK F. I. A, WIDODO J. J. N. WAHAB R. A., 2018. *Characterization, optimization and stability studies on Candida rugose lipase supported on nanocellulose reinforced chitosan prepared from oil palm biomass*, Int. J. Biol. Macromol. 114, 306-315.

ERPEK C. E. Y., OZKOC G., YILMAZER U., 2017. *Comparison of natural halloysite with synthetic carbon nanotubes in poly(lactic acid) based composites*, Polym. Compos. 38, 2337-2346.

GAAZ T. S., SULONG A. B., KADHUM A. A. H., AL-AMIERY A. A., NASSIR M. H., JAAZ A. H., 2017. *The impact of halloysite on the thermo-mechanical properties of polymer composites*, Molecules 22, 838-858.

JESIONOWSKI T., KRYSZTAFKIEWICZ A., 2001. *Influence of silane coupling agents on surface properties of precipitated silicas*, J. Non-Cryst. Solids 277, 45-47.

KADAM A. A., JANG J., LEE D. S., 2017. *Supermagnetically tuned halloysite nanotubes functionalized with aminosilane for covalent laccase immobilization*, ACS Appl. Mater. Interfaces 9, 15492-15501.

KIM H. J., SUMA Y., LEE S. H., KIM J. A., KIM H. S., 2012. *Immobilization of horseradish peroxidase onto clay minerals using soil organic matter for phenol removal*, J. Mol. Cat. B 83, 8-15.

KOLODZIEJCZAK-RADZIMSKA A., JESIONOWSKI T., KRYSZTAFKIEWICZ A., 2010. *Obtaining zinc oxide from aqueous solution of KOH and $Zn(CH_3COO)_2$*, Physicochem. Probl. Miner. Process. 44, 93-102.

KOLODZIEJCZAK-RADZIMSKA A., 2017. *Functionalized Stober silica as a support in immobilization process of lipase from Candida rugosa*, Physicochem. Probl. Miner. Process. 53, 878-892.

KOLODZIEJCZAK-RADZIMSKA A., ZDARTA J., JESIONOWSKI T., 2018. *Physicochemical and catalytic properties of acylase I from Aspergillus melleus immobilized on amino- and carbonyl-grafted Stober silica*, Biotech. Progress, 34, 767-777.

KUMAR-KRISHNAN S., HERNANDEZ-RANGEL A., PAL U., CEBALLOS-SANCHEZ O., FLORES-RUIZ F. J., PROKHOROV E., ARIAS DE FUENTES O., ESPARZA R., MEYYAPPANG M., 2016. *Surface functionalized halloysite nanotubes decorated with silver nanoparticles for enzyme immobilization and biosensing*, J. Mater. Chem. B 4, 2553-2560.

LVOV Y. M., DEVILLIERS M. M., FAKHRULLIN R. F., 2016. *The application of halloysite tubule nanoclay in drug delivery*, Expert. Opin. Drug. Deliv. 5247, 1-10.

MASSARO M., LAZZARA G., MILIOTO S., NOTOA R., RIELA S., 2017. *Covalently modified halloysite clay nanotubes: synthesis, properties, biological and medical applications*, J. Mater. Chem. B 5, 2867-2882.

ORREGO C.E., SALGADO N., VALENCIA J.S., GIRALDO G.I., GIRALDO O.H., CARDONA C.A., 2010. *Novel chitosan membranes as support for lipases immobilization: characterization aspects*, Carbohyd. Polym., 79, 9-16.

PANDEY G., MUNGUAMBE D. M., THARMAVARAM M., RAWTANI D., AGRAWAL Y.K., 2017. *Halloysite nanotubes - an efficient 'nano-support' for the immobilization of α-amylase*, Appl. Clay Sci. 136, 184-191.

TERZOPOULOU Z., PAPAGEORGIOU D. G., PAPAGEORGIOU G. Z., BIKIARIS D. N., 2018. *Effect of surface functionalization of halloysite nanotubes on synthesis and thermal properties of poly(ε-caprolactone)*, J. Mater. Sci. 53, 6519-6541.

TOOGOOD H. S., HOLLONGSWORTH E. J., BROWN R. C., TAYLOR I. N., TAYLOR S. J. C., MCCAUGE R., LITTLECHILD J. A., 2002. *A thermostable L-aminoacylase from thermococcus litoralis: cloning, overexpression, characterization and applications in biotransformations*, Extremophiles 6, 111-122.

TULLY J., YENDLURI R., LVOV Y., 2016. *Halloysite clay nanotubes for enzyme immobilization*, Biomacromolecules 17, 615-621.

YOUSHKO M. I., VAN LANGEN L. M., SHELDON R. A., SVEDAS V. K., 2004. *Application of aminoacylase I to the enantioselective resolution of α-amino acid esters and amides*, Tetrahedron Asymmetr. 15, 1933–1936.

YUAN P., TAN D., ANNABI-BERGAYA F., 2015. *Properties and applications of halloysite nanotubes: recent research advances and future prospects*, Appl. Clay Sci. 112-113, 75-93.

VAIDYA B. K., KUWAR S. S., GOLEGAONKAR S. B., NENE S. N., 2012. *Preparation of cross-linked aggregates of L-aminoacylase via co-aggregation with polyethyleneimine*, J. Mol. Catal. B 74, 184-191.

ZHANG Y., TANG A., YANG H., OUYANG J., 2016. *Applications and interfaces of halloysite nanocomposites,* Appl. Clay Sci. 118, 8-17.

ZHAI R., ZHANG B., LIU L., XIE Y., ZHANG H., LIU J., 2010. *Immobilization of enzyme biocatalyst on natural halloysite nanotubes*, Catal. Commun. 12, 259-263.

ZHU K., DUAN Y., WANG F., GAO P., JIA H., MA C., WANG C., 2017. *Silane-modifed halloysite/Fe_3O_4 nanocomposites simulataneous removal of Cr(VI) and Sb(V) and positive effects of Cr(VI) on Sb(V) adsorption*, Chem. Eng. J. 311, 236-246.